

Laboratori Nazionali di Frascati

LNF-73/14

P. Carelli, I. Modena and F. P. Ricci :
SELF-DIFFUSION IN KRYPTON AT INTERMEDIATE DENSITY

Phys. Rev. A7, 298 (1973).

Self-Diffusion in Krypton at Intermediate Density

P. Carelli* and I. Modena*

Laboratori Nazionali del Comitato Nazionale per l'Energia Nucleare, Frascati, Italy

and

F. P. Ricci

*Istituto di Fisica "G. Marconi," Università di Roma,
and Gruppo Nazionale Struttura della Materia del Consiglio Nazionale delle Ricerche,
Roma, Italy*

(Received 1 May 1972)

The self-diffusion coefficient in Kr has been measured throughout a large range of densities ($0.35 < \rho < 2$ g/cm³) at temperatures near the critical one. The results are compared with molecular-dynamic calculations and with the CH₄ behavior. Although the qualitative agreement is good, disagreement from a quantitative point of view was found. The "normal behavior" of the self-diffusion coefficient in the critical region has been deduced.

INTRODUCTION

At present the "computer experiments"¹ seem to be the most powerful way for investigating the static and the dynamic behavior of the dense fluids. Some of the numerical predictions must, however, be compared with real experiments. This ensures that the hypothesis about the intermolecular potential on which the model is based gives a correct description of the world around us.

Recently a thorough study has been published² on the self-motion of atoms in a Lennard-Jones fluid; the study was carried out using computer experiments. These "experiments" have a range of $0.72 \leq T^* \leq 5.09$ and $0.30 \leq \rho^* \leq 0.85$, where $T^* = k_B T / \epsilon$ and $\rho^* = \rho \sigma^3 / m$ are the reduced temperature and density, ϵ and σ the depth and the core of the Lennard-Jones potential, m the atomic mass, and k_B the Boltzmann constant.

Noble gases Ar, Kr, and Xe are the substances which should be described by a classical Lennard-Jones fluid. The authors² compare the numerical results of the self-diffusion constant with some experiments on Ar³ and claim a very good agreement. However, these experiments cover a small range of densities and temperatures since $0.725 \leq T^* \leq 0.925$ and $0.763 \leq \rho^* \leq 0.835$; that is, the

measurements are only near the triple point. Since suggestions have been made that at intermediate densities many-body forces become important, it is worthwhile to measure the self-diffusion coefficient in Kr for a large range of densities ($0.1 \leq \rho^* \leq 0.7$). Moreover, if the experimental data are taken at a temperature near the critical temperature T_c but outside the critical region [i. e., $(T - T_c / T_c) > 3\%$], we obtain the "normal" behavior of the self-diffusion coefficient in the critical region. This point is quite important since the deduction of an anomalous behavior of the self-diffusion coefficient at the critical point depends upon a good knowledge of the "normal" behavior. This problem has caused erroneous statements in the past.^{4,5} Finally, we wish to point out that extensive measurements are available for the self-diffusion in CH₄⁶ at various temperatures and for $0.07 \leq \rho^* \leq 0.82$.

Since CH₄ is a polyatomic molecule, the comparison between the behavior of Kr and CH₄ will give us an idea of the importance of the internal degrees of freedom in the self-diffusion process.

EXPERIMENTAL APPARATUS

The capillary method of Anderson and Saddington⁷ has been used. Since we were interested in

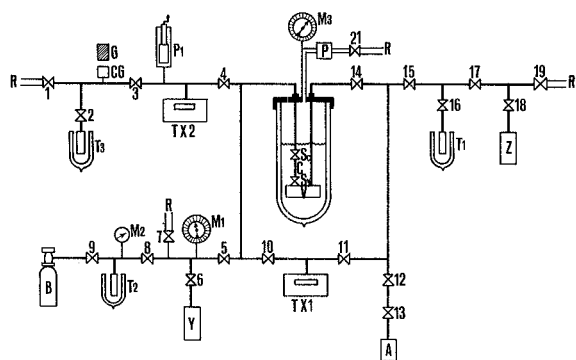


FIG. 1. Block diagram of the experimental apparatus. 1 to 19 are high-pressure valves, B and Y are reservoirs of natural Kr; A is the reservoir containing Kr-Kr⁸⁵ mixture of high concentration of Kr⁸⁵. The mixture to be used in the diffusion experiment is prepared mixing natural Kr from B or Y and radioactive Kr⁸⁵ from A, and then it is stocked in Z. T₁, T₂, and T₃ are cryogenic traps with thick walls so they can hold up to 400 atm. TX1 and TX2 are Texas pressure gauges. M₁, M₂, and M₃ are Bourdon gauges. R are vacuum pumps, P is the bellows manostat. P₁ is a mechanical piston. For the diffusion cell see Fig. 2.

obtaining high densities at temperature near T_c , the apparatus was built to hold pressures up to 400 atm and to perform the diffusion experiments down to the liquid-nitrogen temperature. The block diagram of the whole apparatus is shown in Fig. 1 and details of the diffusing cell are illustrated in Fig. 2. The experiment was carried out as follows.

(i) After evacuating the system and closing SV, the mixture of Kr-Kr⁸⁵ held in the reservoir Z is condensed in the basin V through valve 14. T₁ is used as a cryogenic compressor. The pressure in V is given by TX1.

(ii) After closing SC and opening SV for a short time, a sample of the condensed solution which we call "standard" is taken out. It is transferred through SC, 4, 3, and 2 to T₃. If T₃ is immersed in the liquid nitrogen, it works as a cryogenic pump taking at least 99% of the fluid contained in the capillary: The condensation in T₃ can be followed, since the pressure can be read from TX2. When the condensation is complete, we close valve 4. We warm up T₃ to room temperature, and the sample is transferred to CG (the volume of T₃ is 2% of the volume of CG). The pressure in CG is read using TX2. The piston P₁ changes the volume of the analyzing region and allows the determination of the radioactivity of the gas in CG at the different pressures. The radioactivity of the gas in CG is measured by G.⁹ The vessel CG has an end window, in front of G, made of Mylar, 0.025 mm thick. Since Kr⁸⁵ emits β^- of 0.67 MeV, the absorption by the two windows is negligible. C_s is the specific

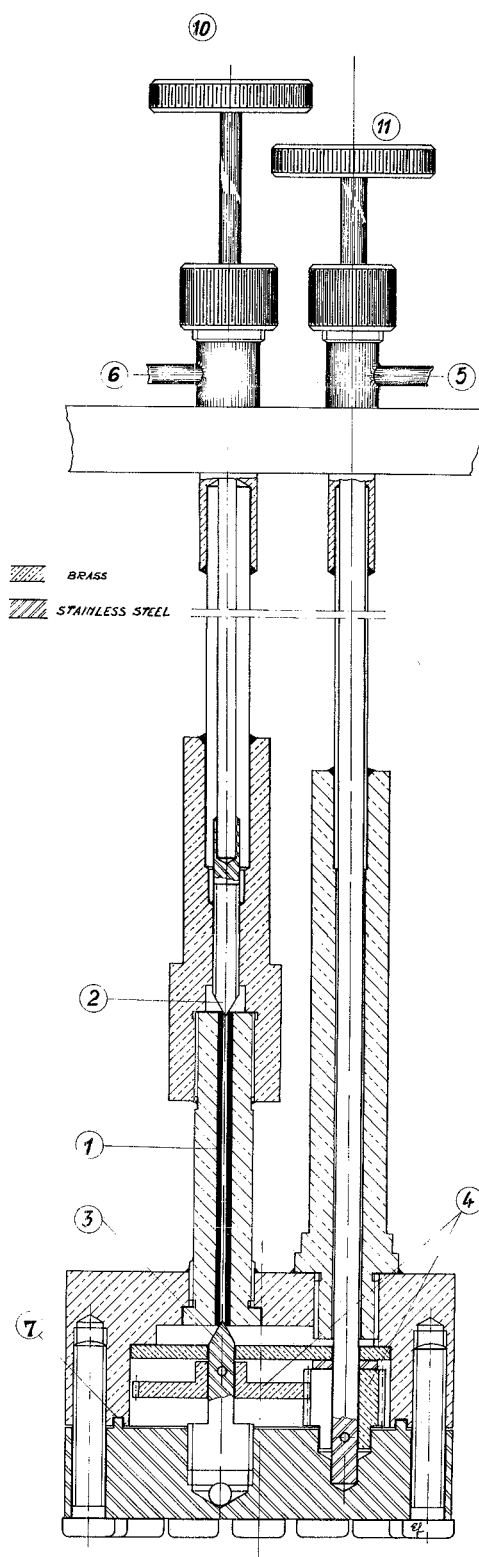


FIG. 2. Diffusion cell: (1) the capillary C (i.d. 0.07 cm; over all length 4.8 cm); (2) needle valve SC of Fig. 1; (3) needle valve SV of Fig. 1; (4) gears; (5) mixture line connecting V with 14 (see Fig. 1); (6) capillary line; (7) indium seal. The actual volume of the basin V, which is filled with the mixture, is 7 cm³.

activity of the standard.

(iii) After evacuating the capillary line, we fill the capillary C with natural Kr from T_2 . The filling pressure is read from M1 and is made equal to the pressure in V, read from TX1. Therefore, the densities in C and V are the same. Then SC is closed.

(iv) SV is opened. At this point the diffusion period begins. To avoid turbulence the opening time is not less than 20 sec. Also, the SV opening system was built in such a way (see Fig. 2) that there is no variation in the basin volume during the opening of SV.

(v) SV is closed. The time between steps 4 and 5 is the diffusion time.

(vi) After evacuating the capillary line, the fluid from C is transferred to CG as in step (ii). However, in this case, the Kr^{85} concentration was not homogeneous along the capillary since there will be a small amount of gas remaining in the capillary line, perhaps with Kr^{85} concentration different from the average; we homogenize the fluid contained in the capillary by moving the piston P_1 up and down after opening SC but before condensing the Kr in T_3 . We control the degree of homogenization by measuring the activity of partial withdrawals of the same sample. We wish to point out that if P_1 is in a fixed position we can derive, from the reading of TX2 (which measures the pressure in CG) the Kr density in which the

diffusion process took place. This pressure is much smaller than one atmosphere even for high-density runs. This method is very convenient and it generally gives the density value within 1%.

This value is in agreement within this 1% limit, with the density value derived from PVT.¹⁰

C_D is the specific activity of the diffusion sample.

(vii) Step (ii) is repeated; this makes it possible to check that the Kr^{85} concentration in V is maintained constant during the diffusion process.

The temperature of the diffusion cell is measured by a Pt thermometer¹¹ with a sensitivity of ± 0.01 °K; this thermometer is held mechanically very tight to the diffusion cell. We also checked that along our diffusion cell the temperature gradients are less than 0.01 °K. This indicates, as does the very good reproducibility of Table I, that we can exclude thermal convection. The temperature control is obtained by regulating the vapor pressure over the CHClF_2 (freon 22) bath by a bellows manostat¹² capable of controlling the pressure to better than 0.4 Torr. This value at 220 °K gives $\Delta T \leq \pm 0.02$ °K. This stability limit is in agreement with the response of the Pt thermometer. As mentioned before, the pressure of Kr in V is read from TX1 which has a precision of 2×10^{-2} atm. The knowledge of the temperature allows us to derive the density using the PVT data available in the literature.¹⁰ Taking into account the errors in T , in p , and in the graphic interpolation of the

TABLE I. Experimental data and D values.

Run	P (atm)	T (°K)	ρ (g/cm ³)	t (sec)	D (cm ² sec ⁻¹)	$D\rho\left(\frac{220}{T}\right)^{0.9}$ (g cm ⁻¹ sec ⁻¹)
1	65.83	232.99	0.46 ± 0.01	1198	5.69 ± 0.34	2.47 ± 0.22
2	64.80	232.97	0.455 ± 0.01	3361	6.08 ± 0.35	2.63 ± 0.21
3	87.45	233.04	0.85 ± 0.01	1799	3.22 ± 0.17	2.60 ± 0.17
4	52.36	222.80	0.367 ± 0.007	1263	6.66 ± 0.65	2.42 ± 0.29
5	71.0	223.3	0.74 ± 0.01	1800	3.69 ± 0.20	2.59 ± 0.17
6	70.37	222.80	0.75 ± 0.01	1319	3.61 ± 0.24	2.69 ± 0.21
7	83.04	218.31	1.307 ± 0.005	2522	1.82 ± 0.09	2.39 ± 0.12
8	82.60	218.34	1.295 ± 0.005	1802	1.93 ± 0.08	2.52 ± 0.11
9	98.88	218.38	1.44 ± 0.01	2411	1.66 ± 0.06	2.41 ± 0.10
10	76.07	218.34	1.185 ± 0.005	3301	2.36 ± 0.12	2.81 ± 0.15
11	72.86	218.36	1.12 ± 0.01	2406	2.47 ± 0.16	2.78 ± 0.20
12	68.88	218.35	0.97 ± 0.01	1804	3.03 ± 0.21	2.96 ± 0.23
13	84.4	210.01	1.533 ± 0.005	3607	1.37 ± 0.07	2.18 ± 0.11
14	85.4	210.08	1.530 ± 0.005	3008	1.29 ± 0.06	2.07 ± 0.10
15	111.28	210.20	1.625 ± 0.005	3005	1.12 ± 0.06	1.89 ± 0.10
16	97.45	199.55	1.74 ± 0.01	3002	0.92 ± 0.04	1.76 ± 0.07
17	94.3	183.6	1.90 ± 0.02	3125	0.615 ± 0.026	1.38 ± 0.06
18	97.35	183.57	1.91 ± 0.02	5703	0.646 ± 0.020	1.45 ± 0.06
19	101.5	222.29	1.409 ± 0.005	2408	1.51 ± 0.07	2.13 ± 0.11
20	82.22	220.25	1.228 ± 0.010	3606	2.04 ± 0.11	2.50 ± 0.15
21	72.89	220.24	1.010 ± 0.005	2403	2.79 ± 0.15	2.82 ± 0.15
22	62.39	220.22	0.570 ± 0.005	1805	4.62 ± 0.39	2.63 ± 0.25
23	70.68	220.18	0.907 ± 0.007	3125	3.37 ± 0.16	3.05 ± 0.17
24	71.20	220.21	0.933 ± 0.010	2703	3.12 ± 0.18	2.92 ± 0.20
25	68.27	220.21	0.791 ± 0.007	1414	3.62 ± 0.40	2.86 ± 0.34

available *PVT* data, we derive the density with a maximum error of 2% at low densities and 0.5% at high densities. These density values agree very well, within the stated errors, with those derived from the measurement of the total amount of the capillary content, as we said in step (vi). For details and drawings on the experimental apparatus, we refer the reader to our internal report LNF 71/33 of the National Laboratory of Frascati.

EXPERIMENTAL RESULTS

The self-diffusion coefficient D can be evaluated by solving the Fick law in the case of a one-dimensional capillary connected to an infinite source¹³:

$$\frac{C_s - C_d}{C_s} = \frac{8}{\pi^2} \sum_{n=0}^{\infty} \frac{1}{(2n+1)^2} \exp\left(-\frac{(2n+1)^2 \pi^2 D t}{4L^2}\right), \quad (1)$$

where L is the effective capillary length (in our case the capillary has a diameter of 0.07 cm and an effective length of 4.6 cm after one corrects for the penetration of SV and SC in C), t is the diffusion time, and C_s and C_d are the activities of the standard and diffusion samples. C_s and C_d are measured in counts per minute per Torr in CG. The counts are corrected for the background and the dead time of the counter. The errors in C_s come from the statistical error of the counts and from the error in the value of the pressure in CG obtained from TX2 (the sensitivity of TX2 is ~ 50 mTorr). The indetermination in the knowledge of the value of L affects the absolute value of D by an error which is smaller than 2%. The error on t is smaller than 0.5% in every run and therefore is negligible with respect to the other errors. The values of D , calculated from Eq. (1), according to our measurements are reported in Table I. Since the errors in C_s , C_d , and ρ increase with the decrease of ρ , we cannot measure D with an accuracy of better than 10% at densities lower than 0.35 g/cm³ using the diffusion cell we have at our disposal.

From Table I we can see the reproducibility of D is very good, even for diffusion times changing by a factor of 3.

Until now, few experimental data on self-diffusion in Kr are available in the literature. In particular, data are given only at room temperature for densities lower than the critical density¹⁴ and at temperatures near the triple point³ for high density. Our data are in good agreement with the literature if the correction for the temperature difference is taken into account.

DISCUSSION

To describe the data of Table I it is necessary to choose the more representative thermodynamic variables. Recently it has been shown¹⁵ that for the transport properties in dense fluids the most

significant thermodynamic variables are density and temperature. Moreover, the dependence on the density is much stronger than the dependence on the temperature. Our self-diffusion data enable us to analyze only the dependence of D on the density. For this reason we prefer to scale these data at exactly the same temperature, i.e., 220 °K. The temperature correction can be made quite confidently using the results either of the molecular-dynamic computations² or of the self-diffusion in CH₄.⁶ In both cases we find that, at least in our range of densities and temperatures, the behavior of D at $\rho = \text{const}$ is of the type $D = AT^{0.9}$, where A is a constant dependent only on the density. This relationship should not be considered a physical law but rather a useful interpolation formula.

Furthermore, we wish to point out that a change in the power of T from 0.7 to 1.1 does not imply a change in the self-diffusion coefficient greater than the experimental error of D . This is true for our case since the temperatures of the various measurements do not differ much from 220 °K.

In Fig. 3 our experimental values of D , reduced at 220 °K, are reported together with those obtained from the molecular-dynamic values¹⁶ given in Table I of Ref. 2. The curve shown in Fig. 3 is the third-order polynomial best fit, which has been reported⁶ to describe the self-diffusion in CH₄. The polynomial¹⁷ has been converted for Kr at 220 °K using the principle of corresponding states.¹⁸

First of all, we want to consider the comparison between our experimental data and the molecular-dynamic results. We see that at high densities the agreement is rather good, as has already been shown for the case of Ar.² At intermediate densities there seems to be a discrepancy outside the experimental errors. Unfortunately, there are not enough data available for the molecular-

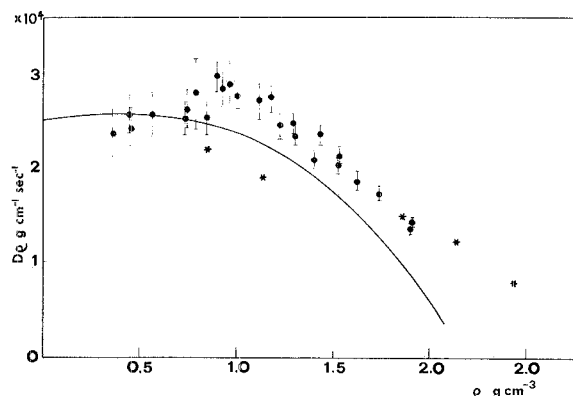


FIG. 3. Self-diffusion in Kr at 220 °K: (1) dots with vertical bar, the experimental results of the present work; (2) stars, results from molecular dynamics as in Table I of Ref. 2; (3) solid line, behavior of self-diffusion following the CH₄ results (Ref. 17).

dynamic calculations in this density region to allow us to establish this discrepancy in a definite way. However, if this disagreement were confirmed, we would have to conclude that it is not correct to use the Lennard-Jones potential for describing a noble-gas fluid in a large range of density.

From the comparison between the behavior of the self-diffusion in Kr and in CH₄ we can see that the qualitative shape is the same. However, from a quantitative point of view there is a progressive disagreement in the high-density region. Also, around the critical density the small bump present in Kr is completely outside the CH₄ behavior.

A very interesting situation has been pointed out by Alder and Wainwright¹⁹ concerning the atomic motion in dense fluids. Analyzing their computer experiments on hard-sphere fluids, they found that at intermediate densities there is an unexpected long persistence of velocity currents which leads to enhanced transport coefficients with respect to the Enskog values. Moreover, analyzing the CH₄ self-diffusion experiments, it has been found²⁰ that the same phenomenon is also present.

The same analysis was made for all the experimental results of the self-diffusion in Kr. In Fig.

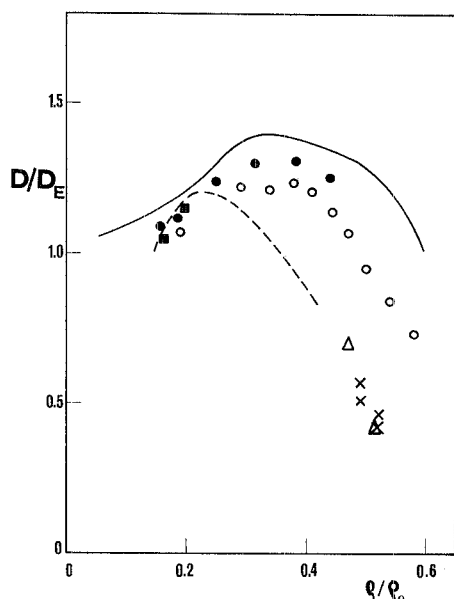


FIG. 4. Ratio of the experimental diffusion coefficient to the Enskog value as a function of density where the density is measured relative to the close-packed density ρ_0 . The solid curve represents the hard-sphere behavior from Fig. 1 or Ref. 20. The dashed line represents the behavior of Kr derived from the best fit of our experimental data. The experimental points for Kr at room temperature, \blacksquare (Ref. 14); and at 125 and 135 °K, \times (Ref. 3); the experimental points for methane at 298.2 °K, \bullet (Ref. 6); and long the liquid branch of the coexistence curve, \circ (Ref. 6); the experimental points for argon at 104 and 95 °K, \triangle (Ref. 3).

4 we report the behavior of the hard spheres and the data for CH₄,⁶ Ar,³ and Kr, all as the ratio of the diffusion coefficient to the Enskog value, as a function of the density.

To evaluate the diffusion coefficient from the Enskog theory in the case of Ar, Kr, and CH₄ we need the effective core sizes which are deduced from equilibrium data within the framework of the van der Waals theory.²⁰ This can be done from a plot of $pV/Nk_B T$ against $1/T$ at a given density. The core size is then determined at that density and at a given temperature from the high-temperature intercept of the slope at the temperature with the known hard-spheres equation of state. The *PVT* data used for Ar are taken from Ref. 21 and those for Kr from Ref. 10; the calculations for CH₄ are available in Fig. 1 of Ref. 20. These values of effective core sizes for Kr turn out to be 3.40 Å at 308.2 °K, 3.45 Å at 222 °K, and 3.50 Å at 125 °K. The values of $g(\sigma)$ have been taken from Monte Carlo calculations.²² Looking at Fig. 4 we can notice the following features.

(a) The experimental points of Ar and Kr fit rather well the same curves as predicted by the principle of corresponding states.

(b) Hard spheres, CH₄, and noble gases behave qualitatively in the same way. For all of them D/D_E , as a function of the density, goes through a maximum greater than 1 at densities greater than the critical density, and then decreases very rapidly in the high-density region.

(c) However, the behavior of hard spheres, CH₄, and noble gases is quantitatively different. The width of the curves decreases and their maximum decreases as well moves towards lower densities as we consider the hard-sphere curve, the CH₄ curve, and the noble-gases curve, respectively.

Three possible reasons can be suggested for these differences: (i) the presence of an attractive part in the intermolecular potential; (ii) the presence of internal degrees of freedom; (iii) a different behavior of the repulsive part of the interatomic potential.

We do not think point (i) is relevant. In fact, although CH₄ and noble gases both have an attractive part in the interatomic potential, we find the same discrepancy between them as between hard spheres and CH₄. Point (ii) also seems to us to be irrelevant, since according to this hypothesis it is not clear why CH₄ must have an intermediate behavior between hard spheres and noble gases. Point (iii) seems to us to be more reasonable. In fact, previous measurements of the pressure dependence of the diffusion coefficient³ have been interpreted in terms of the greater steepness of the repulsive part of the interatomic potential in the CH₄ with respect to noble gases.

Finally we want to note that, looking at Fig. 3,

the "normal behavior" of D for noble gases in the critical region seems to be represented by $D\rho$ slowly increasing with ρ at constant temperature. The choice of the normal behavior as $D\rho = \text{const}$, as found in the CH_4 case,⁶ would imply an underestimation of about 15%. We want to stress that our data have been taken at a temperature 4.76% higher than T_c , which is quite well outside the critical region, as we can deduce from the equilibrium properties²³ and the thermal conductivity measurement.²⁴ As a result no noticeable critical effects are present. On the other hand, we are very near to T_c as far as the temperature dependence of the normal behavior is concerned.

Finally we would like to mention the density expansion of the transport properties. We do not try to fit our data with a polynomial of powers of density. We think that, in order to proceed cor-

rectly with such a development, the behavior of low density must be known very well. Otherwise all the coefficients derived are meaningless.

CONCLUSION

The experimental results of self-diffusion in Kr clearly require more molecular-dynamic calculations for a Lennard-Jones fluid at intermediate range of density. Such calculations are needed both for understanding the possible failure of the two-body potential and for clarifying the situation of vortices in fluids where a Lennard-Jones potential is present. The behavior of polyatomic molecules seems to be different from the behavior of the monatomic molecules only for details. The "normal behavior" in the critical region has been indicated.

*Present address: Laboratorio di Elettronica dello Stato Solido—Via Cineto Romano, 42—00156 Roma, Italy.

¹A. Rahman, *Phys. Rev.* **136**, A405 (1964); *Physics of Simple Fluids*, edited by H. N. V. Temperley, J. S. Rowlinson, and G. S. Rushbrooke (North-Holland, Amsterdam, 1968), Chaps. IV and V.

²D. Levesque and L. Verlet, *Phys. Rev. A* **2**, 2514 (1970).

³J. Naghizadeh and S. A. Rice, *J. Chem. Phys.* **36**, 2710 (1963).

⁴J. D. Noble and M. Bloom, *Phys. Rev. Letters* **14**, 445 (1965); for the criticism see p. 429 or Ref. 6.

⁵I. R. Krichenskij, N. E. Khazanova, and L. R. Linshitz, *Dokl. Akad. Nauk SSSR* **141**, 397 (1961); for criticism see P. Carelli, I. Modena, and F. P. Ricci, *Phys. Letters* **36A**, 261 (1971).

⁶P. H. Oosting and N. J. Trappeniers, *Physica* **51**, 418 (1971).

⁷J. S. Anderson and K. Saddington, *J. Chem. Soc.* **5**, 381 (1949).

⁸The natural Kr has been supplied by Rivoira with a 99.9% purity. Kr⁸⁵ has been supplied by The Radiochemical Centre of Amersham.

⁹G is Geiger-Muller counter tube with end window 2 mg/cm² thick.

¹⁰F. Theewes and R. J. Bearman, *J. Chem. Thermodyn.* **2**, 171 (1970); W. B. Street and A. L. K. Staveley, *J. Chem. Phys.* **55**, 2495 (1971).

¹¹Rosemount platinum resistance thermometer model No. 118G; $R(0^\circ\text{C}) = 100\ \Omega$.

¹²H. White, *Experimental Techniques in Low Temperature Physics* (Oxford U. P., Oxford, England, 1959),

Chap. VII.

¹³J. Crank, *The Mathematics of Diffusion* (Oxford U. P., Oxford, England, 1957), Chap. IV.

¹⁴L. Durbin and R. Kobayashi, *J. Chem. Phys.* **37**, 1643 (1962).

¹⁵P. E. Diller, H. J. M. Henley, and M. Roder, *Cryogenics* **10**, 286 (1970).

¹⁶To use the molecular-dynamics computations for Kr we used the values $\epsilon/k_B = 165^\circ\text{K}$ and $\sigma = 3.65\ \text{\AA}$. These values have been deduced from the critical-point and the triple-point parameters [J. De Boer, *Physica* **14**, 139 (1948)]. They also agree quite well with the values deduced from the second virial coefficient [N. J. Trappeniers, T. Wassenaar, and G. J. Woler, *Physica* **32**, (1966)].

¹⁷The polynomial used, $D\rho = (2.53 + 0.28\rho - 0.21\rho^2 - 0.20\rho^3) \times 10^{-4}$, has been scaled from Ref. 6 with the CH_4 parameters $\epsilon/k_B = 147^\circ\text{K}$ and $\sigma = 3.71\ \text{\AA}$.

¹⁸E. Helfand and S. A. Rice, *J. Chem. Phys.* **32**, 1642 (1960).

¹⁹B. J. Alder and T. E. Wainwright, *Phys. Rev. Letters* **18**, 988 (1967).

²⁰J. H. Dymond and B. J. Alder, *J. Chem. Phys.* **52**, 927 (1970).

²¹A. L. Gosman, thesis (State University of Iowa, 1965) (unpublished).

²²J. A. Barker and D. Henderson, *Mol. Phys.* **21**, 187 (1971).

²³M. Vicentini-Missoni, J. M. H. Levelt Sengers, and M. S. Green, *J. Res. Natl. Bur. Std. A* **73**, 563 (1969).

²⁴A. Michels and J. V. Sengers, *Physica* **28**, 1238 (1962).